FZD2 Promotes TGF-β-Induced Epithelial-to-Mesenchymal Transition in Breast Cancer via Activating Notch Signaling Pathway

Dilihumaer Tuluhong
Nanjing University Medical School https://orcid.org/0000-0002-8176-0428
Tao Chen
Nanjing University Medical School
Jingjie Wang
Nanjing University Medical School
Huijuan Zeng
Guangzhou Medical University
Hanjun Li
Nanjing University Medical School
Wangmu Dunzhu
Nanjing University Medical School
Qiurong Li
Nanjing University Medical School
Shaohua Wang (wangsh_jinling@126.com)
Department of General Surgery, Jinling Hospital, Medical School of Nanjing University, Nanjing, China
https://orcid.org/0000-0003-2981-1416

Primary research

Keywords: breast cancer, FZD2, poor prognosis, EMT, notch signaling pathway

Posted Date: August 21st, 2020

DOI: https://doi.org/10.21203/rs.3.rs-63207/v1

Version of Record: A version of this preprint was published at Cancer Cell International on April 8th, 2021.
See the published version at https://doi.org/10.1186/s12935-021-01866-3.

Abstract

Background

Breast cancer (BC) is one of the commonest female cancers, which is characterized with high incidence. Although treatments have been improved, the prognosis of BC patients in advanced stages remains unsatisfactory. Thus, exploration of the molecular mechanisms underneath BC progression is necessary to find novel therapeutic methods. Frizzled class receptor (FZD2) belongs to Frizzled family, which has been proven to promote cell growth and invasion in various human cancers. The purpose of our study was to detect the functions of FZD2 and explore its mechanism in BC.

Methods

The level of FZD2 was measured in BC tissues by quantitative realtime polymerase chain reaction (qRT-PCR), western blot, immunohistochemistry (IHC) respectively. Cell Counting Kit-8 (CCK-8), standard colony formation, transwell aasays, wound healing and flow cytometry experiments were adopted separately to test cell viability, invasion, migration, apoptosis and cell cycle distribution. Epithelial-mesenchymal transition (EMT) biomarker were determined by using Immunofluorescence assay. Xenograft tumorigenicity assay was performed to assess the effect of FZD2 on tumor growth *in vivo*.

Results

We determined that FZD2 mRNA and protein expression was abundant in BC tissues. Moreover, high level of FZD2 had significant correlation with poor prognosis. *In vitro* functional assays revealed that silencing of FZD2 had suppressive effects on BC cell growth, migration and invasion. Animal study further demonstrated that FZD2 silencing inhibited BC cell growth *in vivo.* In addition, FZD2 induced EMT in BC cells in a transforming growth factor (TGF)-β1-dependent manner. Mechanistically, knockdown of FZD2 led to the inactivation of Notch signaling pathway.

Conclusion

Based on all these data, we concluded that FZD2 facilitates BC progression and promotes TGF-β1-inudced EMT process through activating Notch signaling pathway.

Background

Breast cancer (BC) is considered to be one of the commonest life-threatening cancer types among women. As reported in 2019, BC accounts for 30% among all new female cancer diagnoses [1]. Local recurrence and distant metastasis are the main reasons for the high mortality of BC patients [2]. Although various treatments have been developed for BC patients, the effective therapeutic targets remain limited.

Therefore, exploring the molecular mechanism underneath BC progression is of great significance to develop novel therapeutic strategies.

Frizzled family proteins (FZDs, including FZD1-FZD10) function as cell surface receptors of WNT signaling pathway. Each member of FZDs can activate WNT signaling pathway through interacting with different WNT proteins [3]. As previously reported, FZD2 is dysregulated in various cancer types, such as oral squamous cell carcinoma [4], gastric cancer [5], endometrial cancer [6], hepatocellular carcinoma [7] and tongue squamous cell carcinoma [8]. There is also a study reported that FZD2 suppresses tumor growth in salivary adenoid cystic carcinoma [9]. In addition, non-canonical FZD2 pathway has been recognized to be a regulator for epithelial-to-mesenchymal transition (EMT) and migration [10]. Nevertheless, the mechanism of FZD2 underneath BC progression remains largely unknown.

EMT process is relevant to metastasis and chemotherapy resistance in human cancers [11]. In EMT process, epithelial cells undergo a variety of biochemical alterations and thus change to mesenchymal phenotypes [12]. EMT is closely correlated with the development of human cancers. For example, EMT progress in bladder cancer leads to the high tumor grades and stages [13]. Alterations on the levels of epithelial or mesenchymal markers contribute to the change of EMT process [14]. The expression of EMT markers is tightly associated with the disease progression of SCLCs [15]. Importantly, expression changes of EMT markers are also correlated with BC progression [16].

TGF-β family is a group of cytokines that can act on EMT process in cancer progression [17]. TGF-β1 promotes the acquisition of a mesenchymal phenotype and thus promotes cell invasion and migration [18]. Notch signaling pathway is primarily functions by controlling cell fate decisions, differentiation, and proliferation [19]. According to previous studies, Notch signaling pathway can also involve in EMT process in several different cancer types, such as lung cancer, pancreatic cancer and breast cancer [20–22].

To summarize, this study focused on the functions of FZD2 in BC progression and its regulatory effects on TGF-β1-inudced EMT and Notch signaling pathway.

Materials And Methods

Tissue samples

Primary invasive ductal carcinomas tissues and adjacent normal tissues were obtained from female patients at the Jinling Hospital, affiliated with the Medical School of Nanjing University. All participants didn’t receive neoadjuvant therapies before the operation. A total of 147 female patients participated in this study. The written informed consent had been collected from patients before the study. The investigation was approved by the ethics committee of Jinling Hospital.

Cell Culture And Treatment

SK-BR-3, MCF-7 and MDA-MB-231 cell lines used in this study were obtained from the Type Culture Collection of the Chinese Academy of Sciences (Shanghai, China). MCF-10A (normal human mammary epithelial cell line) purchased from KeyGEN Biotech Company (Nanjing, China) was used as the control cell line. All cell lines were grown in Dulbecco's Modified Eagle's medium (DMEM, KeyGEN) in which 10% fetal bovine serum (A3160801, Gibco) and 1% penicillin-streptomycin were added. Cell culture was accomplished in a humidified incubator containing 5% CO_2 at 37 °C. Cell passage was performed when the confluence reached to 90%. Reagents used in this study, including TGF-β1 and TGF-β type I Receptor inhibitor SB431542, were separately purchased from PeproTech (#100 – 21, USA) and MedChemExpress (HY-10431, USA).

Sirna Transfection

siRNAs targeting FZD2 were designed and synthesized by Ribobio (Guangzhou, China).. For the silencing of FZD2, siRNAs were transfected into SK-BR-3 and MDA-MB-231 cells in accordance with the instruction manual for Lipofectamine 3000 (Invitrogen, #L3000015, Carlsbad, CA, USA). Plasmid amplification was accomplished through transformation and pumping. The levels of FZD2 mRNA and protein were separately checked by qRT-PCR and western blot. Sequences for all siRNAs are as follows:

si-FZD2-1	**CATCCTATCTCAGCTACAA**
si-FZD2-2	CCATCATGCCCAACCTTCT
si-FZD2-3	CCCGATGGTTCCATGTTCT

Rna Extraction And Qrt-pcr

Total RNA was extracted from tissues with RNA kit (Promega), whereas those extracted from cells were accomplished with TRIzol (Invitrogen). RNA was reverse transcribed into cDNA using PrimeScript RT Master Mix (Perfect Real Time, TaKaRa, Shiga, Japan) and then analyzed by qRT-PCR with SYBR Green Master Mix on an Applied biosystem 7500 machine (USA). $2^{-\Delta\Delta CT}$ method was used to calculate relative mRNA expression by normalizing to GAPDH. Sequences for all primers used for qRT-PCR were provided in Table 1.

Table 1
Primer sequences for qPCR primers

E-cadherin	**Forward:5'-ATGCCGCCATCGCTTACAC-3'**
	Reverese:5'-GGTGACCACACTGATGACTCCTG-3'
Fibronectin	Forward:5'-TGCCAACCTTTACAGACCTATCC-3'
	Reverese:5'-GCTGACTCGGAGTCTCAGTGATA-3'
FZD2	Forward:5'-ATCTCTGGCGTTCAGGTTAGCA-3'
	Reverese:5'-CCACCCGTCTTTATCACTTTTTG-3'
GAPDH	Forward:5'-GCACCGTCAAGGCTGAGAAC-3'
	Reverese:5'-TGGTGAAGACGCCAGTGGA-3'
N-cadherin	Forward:5'-CGGAGATCCTACTGGACGGT-3'
	Reverese:5'-CCTTGGCTAATGGCACTTGAT-3'
TGF-β1	Forward:5'-CCCACAACGAAATCTATGACAAG-3'
	Reverese:5'-AGAGCAACACGGGTTCAGGT-3'
Vimentin	Forward:5'-CTGGATTCACTCCCTCTGGTT-3'
	Reverese:5'-TCGTGATGCTGAGAAGTTTCGTT-3'
FZD2, frizzled class receptor 2; TGF-β1, transforming growth factor-β1.	

Western Blot

RIPA buffer (Beyotime) was used for extraction of total protein from tissues and cells. BCA Protein Assay Kit (KeyGen Biotech, Nanjing, China) was applied to measure the protein concentration. After resolved on SDS-PAGE, the protein lysates were transferred onto a polyvinylidene fluoride (PVDF) membrane (Immobilon, USA). After blocked in 5% non-fat milk, the membranes were incubated with primary antibodies at 4 °C overnight. After washing, the membranes were incubated with a secondary antibody against rabbit (1: 5000, Abcam) at 37 °C for 1 h. Primary antibodies used in this experiment were shown in Table 2. The blots were detected by the ECL (NCM Biotech, China) method.

Table 2
Primary antibodies for western blot analysis

Name	Company	Catalog Number	Dilution
BAX	Proteintech	50599-2-Ig	1:4000
BCL2	Proteintech	12789-1-AP	1:1000
Caspase3	CST	#9662	1:1000
E-cadherin	Proteintech	20874-1-AP	1:5000
FZD2	Proteintech	24272-1-AP	1:500
Fibroactin	Proteintech	15613-1-AP	1:500
GAPDH	CST	#2118	1:1000
Hes1	CST	#11988	1:1000
Notch1	CST	#3608	1:1000
N-cadherin	Proteintech	22018-1-AP	1:2000
P21	Proteintech	10355-1-AP	1:500
TGF-β	Proteintech	21898-1-AP	1:1000
Vimentin	Proteintech	10366-1-AP	1:3000

CST, Cell signaling technology; FZD2, frizzled class receptor 2; TGF-β1, transforming growth factor-β1.

Immunohistochemistry (ihc)

hesFor IHC staining, sections were dewaxed with xylene and rehydrated in ethanol. To avoid non-specific staining, samples were washed with PBS and blocked with 5% BSA at room temperature for 30 min. After washing, sections were incubated with primary antibodies against FZD2 (1:50, Abcam), TGF-β1 (1:500, Proteintech), Ki-67 (1:10000, Proteintech) at 4 °C overnight. Afterwards, sections were incubated with secondary antibody kit SP0031 and/or SP0021 (Solarbio, China) in accordance with the instruction manual. Images were taken under a microscope (Olympus CX41, Japan).

Evaluation Of Staining Of Tissue Slides

After immunostaining, FZD2 in different tissues was evaluated by a semi-quantitative immunoreactivity scoring system (IRS). The indexes of Immunostaining intensity were separated as 0 (no immunostaining), 1 (weak), 2 (moderate) and 3 (strong). The scores for immunoreactive cells were separately defined as 0 (no immunoreactive cells), 1 (less than10%), 2 (between 10% and 50%), 3 (between 51% and 80%) and 4 (more than 80%). The IRS index for each case ranges from 0 to 12. FZD2

was considered to be upregulated in cases with 6 or higher IRS score, whereas FZD2 was considered to be downregulated in those with IRS score less than 6.

Cell Counting Kit 8 (cck-8) Assay

The transfected cells were plated into 96-well plates at 6–8 × 10^3 cells per well in 100 μL cell suspension. After added CCK-8 solution (10 μL) (Dojindo, Kumamoto, Japan) at six different time points (0 h, 24 h, 48 h, 72 h, 96 h, 120 h), cells were incubated at 37 °C for 2 h. Finally, a microplate reader was applied to measure the absorbance at 450 nm (OD 450 nm).

Colony Formation Assay

The transfected cells were seeded in 6-well plates at 3 × 10^3 cells per well and cultured in DMEM containing 10% FBS. At day 14, cells were fixed with methanol for 10 min and stained by 0.1% crystal violet for 15 min. After captured the pictures, the number of colonies was recorded manually.

Cell Migration And Invasion Assays

Matrigel-coated 24-well Transwell chambers (Corning Incorporated, Corning, NY, USA) and non-coated Transwell chambers (#353097; BD Biosciences, USA) were separately used for cell invasion assay and cell migration assay. Twenty-four hours after transfection, the cells were plated into the upper compartment containing serum-free DMEM at a density of 2 × 10^4 cells per well. The lower chamber was added with DMEM containing 20% FBS. Forty-eight hours later, the cells in the upper chamber were removed with cotton swabs, while the cells on the lower surface were fixed with 4% paraform-aldehyde for 10 min and stained with 0.1% crystal violet for 15 min. The results were obtained using an inverted microscope (Olympus, Japan).

Wound Healing Assay

Twenty-four hours after siRNA transfection, cells were seeded in 6-well plates at a density of 1 × 10^6 cells each well. After cell attachment, a scratch was created with a 200 μL pipette tip in the cell layer. Cells that had been scraped off were washed away with PBS. Forty-eight hours later, the distance of wound was measured by observing images at 0 h and 48 h.

Flow Cytometry Analysis Of Cell Cycle Distribution

Twenty-four hours after siRNA transfection, cells were plated into 6-well plates at a density of 1 × 10^6 cells per well. Next, cells were rinsed in prepared phosphate buffer saline (PBS). After incubated with the

propidium iodide (KeyGEN, China), flow cytometry was applied to detect the cell population at different phase (G0/G1, S and G2/M). Percent of cells in different phases was measured by BD FACSCantoII (BD Biosciences, USA).

Flow Cytometry Analysis Of Cell Apoptosis

Twenty-four hours after siRNA transfection, EDTA-free trypsin (Beyotime, China) was used to digest the cells, and 1×10^6 cells/ml were counted. Cell apoptosis assay was processed under the FITC Annexin V Apoptosis Detection Kit (BD Biosciences), cell apoptosis was detected by BD FACSCanto II (BD Biosciences).

Immunofluorescence Microscopy

Cells were fixed in parafolmaldehyde (4%) for 20 min and permeabilized with 0.5% Triton X-100 in PBS for 10 min. Cells were blocked with PBS/BSA 5% for 30 min. The membranes were incubated with primary antibody against E-cadherin and Vimentin (1: 50, proteintech) at 4 °C overnight. After washing, the membranes were incubated with green-fluorescence conjugated Affinipure antibody (Coralite 488, diluted 1:100, Proteintech) or Red-fluorescence conjugated Affinipure antibody (Coralite 594, diluted 1:100, Proteintech). After washing, DAPI (Sigma, Cat# D-9542) was used for the nuclei staining. Images were visualized using a Nikon ECLIPSE NI (Japan) microscope.

Xenograft Tumorigenicity Assay

For animal study, female BALB/c nude mice (4 weeks old) were bought from the Comparative Medicine Department of Jinling Hospital. Mice were randomly divided into two groups (n = 6 per group) after the tumor volume reached $100mm^3$. si-FZD2-2 and si-NC(Ribobio, China) was administered by intratumoral injection at a dose of 30 μL/piece, administered once every 3 days and continuously for 14 times. Forty days after injection, all mice were killed and the tumors were removed. Tumor tissues were embedded in paraffin for further analyses. Animal study was conducted followed the protocol of the animal ethics committee of Jinling Hospital.

Tunel Assay

Apoptosis in tumor tissues removed from nude mice was detected by using the TUNEL assay kit (Roche, USA) according to the manufacturer's guidelines.

Statistical analysis

Statistical significance of differences was analyzed with two-tailed student's *t* test (between two groups) or one-way/two-way ANOVA (among multiple groups). All experimental data were obtained from three or more independent experiments and shown as mean ± SD (standard deviation). The correlation between FZD2 expression and the clinicopathological characteristics of BC patients was analyzed using the Chi-squared test. SPSS v17.0 (SPSS Inc., Chicago, IL, USA) and Prism v8.0 (GraphPad, San Diego, CA, USA) were utilized for statistical analyses. Data were statistically significant when *p* values less than 0.05.

Results

FZD2 is significantly upregulated in BC tissues and associated with poor prognosis

According to UALCAN [23] dataset, FZD2 expression is associated with various tumors (Fig. 1A). Based on TCGA dataset, the prognostic value of FZD2 in 701 BC patients was analyzed (Fig. 1B). After analysis, FZD2 overexpression was identified to be correlated with worse distant metastasis free survival (DMFS) indicating the potential involvement of FZD2 in cancer progression. Searching from ONCOMINE database(http://www.oncomine.org/resource/login.html),we identified the upregulation of FZD2 in BC tissues (Fig. 1C).Then, we performed qRT-PCR to examine FZD2 mRNA expression in 42 BC tissues relative to adjacent normal tissues. Not surprisingly, FZD2 presented a higher expression in BC tissues (Fig. 1D). The protein level of FZD2 exhibited the same tendency in BC tissues, as evidenced by western blot analysis (Fig. 1F). IHC revealed that FZD2 was mainly expressed in the cytoplasm (Fig. 1E). Weak staining (+), moderate staining (++) and strong staining (+++) were separately 28 cases, 43 cases and 34 cases. Simultaneously, we found that patients with higher FZD2 expression exhibited significantly poorer OS and DMFS than those with lower FZD2 level (Fig. 1G). Finally, we divided the 105 patients into high and low level of FZD2 expression groups and analyzed the relationship between FZD2 expression and clinical characteristics (Table 3). Overexpression of FZD2 had significant correlations with TNM stages ($p = 0.006$), lymph-node metastasis ($p = 0.024$) and organ metastasis($p = 0$). Overall, highly expressed FZD2 in BC patient samples is correlated with poor prognosis.

Table 3
The association between FZD2 expression and clinical-pathological characteristics in breast cancers

Expression of FZD2			
Factors	**Low(N = 71)**	**High(N = 34)**	**P-value**
Age(y)			
≤ 50	35	17	1
> 50	36	17	
Tumor Size(cm)			
< 2.5 cm	31	22	0.060
≥ 2.5 cm	40	12	
ER Status			
(+)	35	23	0.095
(-)	36	11	
PR Status			
(+)	44	20	0.832
(-)	27	14	
Her-2 Status			
(+)	22	13	0.511
(-)	49	21	
Ki-67 Status (%)			
≤ 20%	24	10	0.824
> 20%	47	24	
Pathological grading			
□-□	51	23	0.655
□	20	11	
TNM Stage			
□-□	57	18	0.006*

*P < .05 was considered statistically significant.

Abbreviations: ER, estrogen receptor; FZD2, frizzled class receptor 2; Her-2, human epidermal growth factor receptor 2; PR, progesterone receptor.

Expression of FZD2			
□-□	14	16	
Lymph-node metastasis			
pN0	54	18	0.024*
pN+	17	16	
Organ metastasis			
No	65	15	0.000*
Yes	6	19	
*P < .05 was considered statistically significant.			
Abbreviations: ER, estrogen receptor; FZD2, frizzled class receptor 2; Her-2, human epidermal growth factor receptor 2; PR, progesterone receptor.			

FZD2 promotes BC cell growth, migration and invasion, while induces cell apoptosis in vitro

Furthermore, we investigated FZD2 expression in BC cells through comparing with the normal MCF-10A cell. As expected, FZD2 was upregulated in three BC cells (Fig. 2A), among which SK-BR-3 and MDA-MB-231 presented the highest FZD2 level ($p < 0.01$). We thus selected these two cells for loss-of-function experiments. At first, silencing FZD2 was confirmed in SK-BR-3 and MDA-MB-231 cells through qRT-PCR and western blot analyses (Fig. 2B). Since si-FZD2-1 and siFZD2-2 resulted in the most significant knockdown effect on FZD2, we used these two siRNAs for subsequent experiments. FZD2 silencing dramatically reduced cell proliferation (Fig. 2C-D). Moreover, cells were arrested at G2/M phase after FZD2 knockdown (Fig. 2E). Therefore, we confirmed that FZD2 promotes *in vitro* cell growth in BC. As for apoptosis, flow cytometry analysis and western blot were conducted in FZD2-silenced BC cells. Then, we observed an enhanced apoptosis rate in cells with FZD2 silencing (Fig. 2F). Consistently, the levels of Bax and cleaved caspase 3 were increased, whereas the level of Bcl-2 was decreased in FZD2-downregulated BC cells (Fig. 2G). The mobility of BC cells was evaluated after FZD2 depletion. Intriguingly, knockdown of FZD2 weakened the migratory and invasive ability of BC cells (Fig. 2H-I). Accordingly, we identified the important role of FZD2 in regulating BC cell migration, invasion and apoptosis *in vitro*.

Fzd2 Silencing Suppresses Bc Cell Growth In Vivo

Animal models were established to investigate the effect of FZD2 silencing on tumor growth. Forty days after injection, we observed the smaller tumor size in si-h-FZD2 group than those in si-NC group (Fig. 3A). The volume and weight of tumors in two groups presented the consistent tendencies (Fig. 3B-C). IHC showed that Ki-67 and TGF-β1 positivity was lower in tumor tissues of si-h-FZD2 group (Fig. 3D). Through TUNEL assays, we confirmed that FZD2 silencing induced apoptosis *in vivo* (Fig. 3D). In the meantime, the levels of Bax and cleaved caspase 3 (pro-apoptotic proteins) were increased, whereas the

level of Bcl-2 (an anti-apoptotic protein) was decreased in response to FZD2 silencing (Fig. 3E). Taken together, FZD2 silencing inhibits BC cell growth *in vivo*.

Depletion of FZD2 reverses EMT process through inactivating Notch signaling pathway

GSEA database illustrated that FZD2 may regulate the Notch signaling pathway (Fig. 4A). To analyze whether FZD2 had the potential to affect EMT process, the expression of EMT markers (E-cadherin, N-cadherin, Vimentin and Fibronectin) was assessed in FZD2-silenced cells. As presented in Fig. 5B-C, the levels of E-cadherin mRNA and protein were enhanced by FZD2 knockdown, whereas N-cadherin, Vimentin and Fibronectin were remarkably downregulated after silencing of FZD2 (Fig. 4B-C). Simultaneously, we measured the levels of Notch pathway-related molecules (Notch1, P21 and Hes1). Intriguingly, FZD2 depletion led to the downregulation of these three proteins (Fig. 4B). At last, Immunofluorescence analysis further revealed that the level of E-cadherin was increased but the level of N-cadherin was decreased in cells with FZD2 knockdown (Fig. 4D). All these data indicated that FZD2 regulates cellular processes in BC potentially through activating Notch signaling.

FZD2 positively regulates TGF1-β in BC cells through Notch signaling pathway

TGF-β signaling plays an essential role in inducing EMT in different types of tumors. According to the data of GEPIA database, TGF-β1 had positive expression correlation with FZD2 or Notch1 in BC patient samples (Fig. 5A). Moreover, the level of TGF-β1 protein was decreased in FZD2-silenced cells (Fig. 5B). Subsequently, the levels of Fibronetin, N-cadherin and Vimentin were significantly increased by the strengthened TGF-β1 in BC cells, whereas the levels of E-cadherin were remarkably decreased (Fig. 5C-D). Meanwhile, the levels of Notch signaling pathway-related proteins were also induced after TGF-β1 treatment in BC cells (Fig. 5C). In addition, TGF-β1-induced protein levels of fibronectin, N-cadherin and Vimentin were reduced again by introducing TGF-β receptor antagonist SB431542 (Fig. 5E), and then the mRNA level of E-cadherin decreased by TGF-β1 was also recovered by SB431542 (Fig. 5F). These findings illustrated that FZD2 promotes BC progression and involves in TGF-β-induced EMT through activating Notch signaling pathway.

Discussion

Accumulating studies have demonstrated that FZDs can involve in the canonical or non-canonical WNT pathway [24]. Notably, FZDs can also be intertwined with other signaling cascades. For example, FZD2 can function as a regulator in EMT and metastasis through Fyn/Stat3 pathway [10]. According to previous studies, FZDs can exert various biological functions in different human cancers. For example, FZD1 silencing induces a strong decrease of MDR1 expression to enhance drug resistance in neuroblastoma (NB) [25]. FZD3 protein expression has close association with the progression of colorectal cancer [26]. High FZD8 expression in human BC tissues is correlated with lymph node metastasis [27]. In our study, FZD2 was identified to be expressed in BC tissues at a significant high level. Importantly, we analyzed the significant correlation between high FZD2 level and the poor prognosis of BC patients. Functionally, FZD2 knockdown led to the inhibition on BC cell growth. Furthermore, silencing

of FZD2 had suppressive effects on both migration and invasion of BC cells. Therefore, we confirmed that FZD2 exerts oncogenic role in BC.

Recently, studies have revealed the involvement of EMT in promoting the malignant development of human tumors [28–30]. To date, evidence has indicated that EMT phenomenon favors the distant metastases in epithelial cancers, including breast cancer [31]. FZDs have also been reported as regulators for EMT process in human cancers. For instance, FZD4 promotes the formation of EMT phenotypes in prostate cancer [32]. SOX8- and SOX9-induced upregulation of FZD7 regulates EMT in TSCC [33] and HCC [34]. In the current study, FZD2 was verified to be a positive regulator for the EMT process of BC cells. Accumulating studies have suggested that TGF-β promotes metastasis in human cancers, including BC [35]. In the present study, we determined that FZD2 positively regulated TGF-β1 expression in BC cells. Furthermore, TGF-β1 promoted EMT process in BC cells, whereas the effect could be reversed by the suppression of TGF-β1 using SB431542. Critically, the positive expression correlation between TGF-β1 and FZD2 was verified in clinical BC samples. Hereto, we confirmed that FZD2 induces EMT in BC in a TGF-β1-dependent manner.

Notch signaling pathway plays an important role in several human malignancies [36]. In addition, Notch signaling pathway is also known as a modulator for EMT process in several different cancer types [21, 37]. In this work, we found that FZD2 may contribute to BC development by modulating Notch signaling pathway.

In conclusion, our findings revealed that FZD2 plays an oncogenic role in BC progression. Mechanistically, FZD2 regulates BC progression and EMT process through modulating TGF-β1 signaling and Notch signaling pathway. Our research findings may help to provide an effective therapeutic target for human BC patients.

Abbreviations

BC
Breast cancer; EMT:epithelial-mesenchymal transition; FZD:frizzled class receptor; IHC:immunohistochemistry; TGF-β1:transforming growth factor-β.

Declarations

Ethics approval and consent to participate

The tissues collected from patients and animal study was approved by the ethics committee of Jinling Hospital and conducted followed the protocol of the animal ethics committee of Jinling Hospital.

Consent for publication

Not applicable.

Availability of data and materials

The datasets used and/or analysed during the current study are available from the corresponding author on reasonable request

Competing interest

The authors declare no conflict of interest.

Funding

This study was supported in part by grants from Science and Technology Program of Nanjing (201605003) and Military Construction Project of National Clinical key Specialty (2014ZDZK002).

Author Contributions

Conceptualization, DilihumaerTuluhong; Data curation, DilihumaerTuluhong; Formal analysis, Tao Chen and Jingjie Wang; Investigation, Jingjie Wang, Hanjun Li and WangmuDunzhu; Methodology, Huijuan Zeng; Resources, Huijuan Zeng; Software, Tao Chen; Supervision, Qiurong Li and Shaohua Wang; Writing – original draft, DilihumaerTuluhong.

Acknowledgement

All authors were major contributors in the writing of the manuscript. We are grateful to all researchers of enrolled studies.

References

1. Siegel RL, Miller KD, Jemal A. Cancer statistics, 2020. CA Cancer J Clin. 2020;70(1):7–30.
2. DeSantis CE, et al. Breast cancer statistics, 2019. CA Cancer J Clin. 2019;69(6):438–51.
3. Zeng CM, Chen Z, Fu L. *Frizzled Receptors as Potential Therapeutic Targets in Human Cancers*. Int J Mol Sci, 2018. 19(5).
4. Zhang E, et al. Frizzled2 mediates the migration and invasion of human oral squamous cell carcinoma cells through the regulation of the signal transducer and activator of transcription-3 signaling pathway. Oncol Rep. 2015;34(6):3061–7.
5. Tomizawa M, et al. Gastric cancer cell proliferation is suppressed by frizzled-2 short hairpin RNA. Int J Oncol. 2015;46(3):1018–24.
6. Bian Y, et al. Promotion of epithelial-mesenchymal transition by Frizzled2 is involved in the metastasis of endometrial cancer. Oncol Rep. 2016;36(2):803–10.
7. Ou H, et al. Frizzled 2-induced epithelial-mesenchymal transition correlates with vasculogenic mimicry, stemness, and Hippo signaling in hepatocellular carcinoma. Cancer Sci. 2019;110(4):1169–82.

8. Huang L, et al. FZD2 regulates cell proliferation and invasion in tongue squamous cell carcinoma. Int J Biol Sci. 2019;15(11):2330–9.
9. Ding LC, et al. FZD2 inhibits the cell growth and migration of salivary adenoid cystic carcinomas. Oncol Rep. 2016;35(2):1006–12.
10. Gujral TS, et al. A noncanonical Frizzled2 pathway regulates epithelial-mesenchymal transition and metastasis. Cell. 2014;159(4):844–56.
11. Dongre A, Weinberg RA. New insights into the mechanisms of epithelial-mesenchymal transition and implications for cancer. Nat Rev Mol Cell Biol. 2019;20(2):69–84.
12. Lu W, Kang Y. Epithelial-Mesenchymal Plasticity in Cancer Progression and Metastasis. Dev Cell. 2019;49(3):361–74.
13. Baumgart E, et al. Identification and prognostic significance of an epithelial-mesenchymal transition expression profile in human bladder tumors. Clin Cancer Res. 2007;13(6):1685–94.
14. Kalluri R, Weinberg RA. The basics of epithelial-mesenchymal transition. J Clin Invest. 2009;119(6):1420–8.
15. Prudkin L, et al. Epithelial-to-mesenchymal transition in the development and progression of adenocarcinoma and squamous cell carcinoma of the lung. Mod Pathol. 2009;22(5):668–78.
16. Khaled N, Bidet Y. *New Insights into the Implication of Epigenetic Alterations in the EMT of Triple Negative Breast Cancer*. Cancers (Basel), 2019. 11(4).
17. Hua W, et al., *TGFbeta-induced metabolic reprogramming during epithelial-to-mesenchymal transition in cancer*. Cell Mol Life Sci, 2019.
18. Hao Y, Baker D, Ten Dijke P. *TGF-beta-Mediated Epithelial-Mesenchymal Transition and Cancer Metastasis*. Int J Mol Sci, 2019. 20(11).
19. Li L, et al. Notch signaling pathway networks in cancer metastasis: a new target for cancer therapy. Med Oncol. 2017;34(10):180.
20. Bao B, et al. Notch-1 induces epithelial-mesenchymal transition consistent with cancer stem cell phenotype in pancreatic cancer cells. Cancer Lett. 2011;307(1):26–36.
21. Yuan X, et al. Notch signaling and EMT in non-small cell lung cancer: biological significance and therapeutic application. J Hematol Oncol. 2014;7:87.
22. Zhang J, et al. NUMB negatively regulates the epithelial-mesenchymal transition of triple-negative breast cancer by antagonizing Notch signaling. Oncotarget. 2016;7(38):61036–53.
23. Chandrashekar DS, et al. UALCAN: A Portal for Facilitating Tumor Subgroup Gene Expression and Survival Analyses. Neoplasia. 2017;19(8):649–58.
24. Ng LF, et al., *WNT Signaling in Disease.* Cells, 2019. 8(8).
25. Flahaut M, et al. The Wnt receptor FZD1 mediates chemoresistance in neuroblastoma through activation of the Wnt/beta-catenin pathway. Oncogene. 2009;28(23):2245–56.
26. Wong SC, et al. Clinical significance of frizzled homolog 3 protein in colorectal cancer patients. PLoS One. 2013;8(11):e79481.

27. Jiang Q, et al. MicroRNA-100 suppresses the migration and invasion of breast cancer cells by targeting FZD-8 and inhibiting Wnt/beta-catenin signaling pathway. Tumour Biol. 2016;37(4):5001–11.
28. Zhou ZJ, et al. HNRNPAB induces epithelial-mesenchymal transition and promotes metastasis of hepatocellular carcinoma by transcriptionally activating SNAIL. Cancer Res. 2014;74(10):2750–62.
29. Shioiri M, et al. Slug expression is an independent prognostic parameter for poor survival in colorectal carcinoma patients. Br J Cancer. 2006;94(12):1816–22.
30. Mahmood MQ, et al. Epithelial mesenchymal transition (EMT) and non-small cell lung cancer (NSCLC): a mutual association with airway disease. Med Oncol. 2017;34(3):45.
31. Wu Y, Sarkissyan M, Vadgama JV. *Epithelial-Mesenchymal Transition and Breast Cancer.* J Clin Med, 2016. 5(2).
32. Gupta S, et al. FZD4 as a mediator of ERG oncogene-induced WNT signaling and epithelial-to-mesenchymal transition in human prostate cancer cells. Cancer Res. 2010;70(17):6735–45.
33. Xie SL, et al. SOX8 regulates cancer stem-like properties and cisplatin-induced EMT in tongue squamous cell carcinoma by acting on the Wnt/beta-catenin pathway. Int J Cancer. 2018;142(6):1252–65.
34. Leung CO, et al. Sox9 confers stemness properties in hepatocellular carcinoma through Frizzled-7 mediated Wnt/beta-catenin signaling. Oncotarget. 2016;7(20):29371–86.
35. Zarzynska JM. Two faces of TGF-beta1 in breast cancer. Mediators Inflamm. 2014;2014:141747.
36. Radtke F, Raj K. The role of Notch in tumorigenesis: oncogene or tumour suppressor? Nat Rev Cancer. 2003;3(10):756–67.
37. Natsuizaka M, et al. Interplay between Notch1 and Notch3 promotes EMT and tumor initiation in squamous cell carcinoma. Nat Commun. 2017;8(1):1758.

Figures

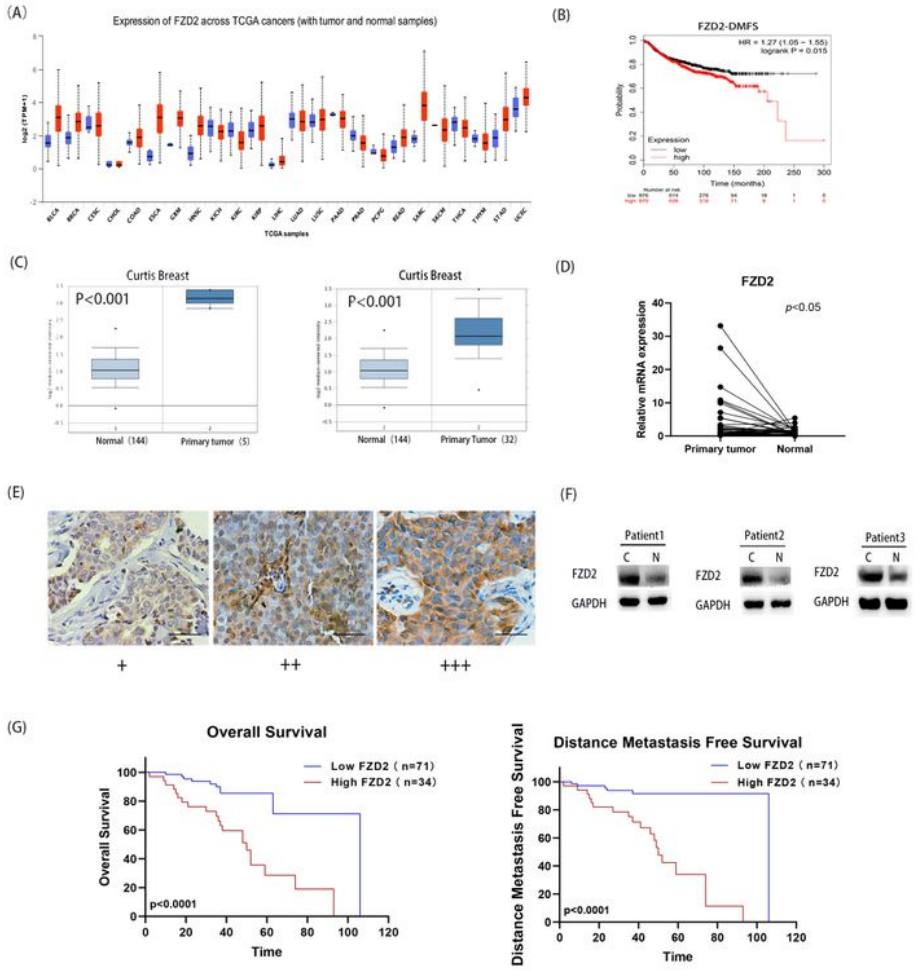

Figure 1

Upregulation of FZD2 in BC tissues is correlated with poor prognosis. (A) Data obtained from TCGA database revealed the FZD2 expression in different types of cancertissues. (B) DMFS of BC patients with high or low level of FZD2 were analyzed by generating KM plots based on publicly available microarray data. (C) Representative images of FZD2 upregulation in BC tissueswere generated from the ONCOMINE database. (D) qRT-PCR detected the mRNA level of FZD2 in 42BC tissues and adjacent normal tissues. (E)

Representative images of FZD2 expression in BC tissueswere obtained using IHC(Original magnification, ×400, scale bar, 100 μm). (F) Western blot analysis of FZD2 protein in BC tissues with adjacent normal tissues as controls. (G) OS (left panel) and DMFS (right panel) in BC patients were analyzed byKM method. *p< 0.05, **p< 0.01, ***p< 0.001wasa symbol of statistical significance. TCGA, the cancer genome atlas; FZD2, frizzled class receptor 2; BC,breast cancer; KM, Kaplan-Meier; OS, overall survival; RFS,recurrence-free survival; DMFS, distant metastasis free survival;

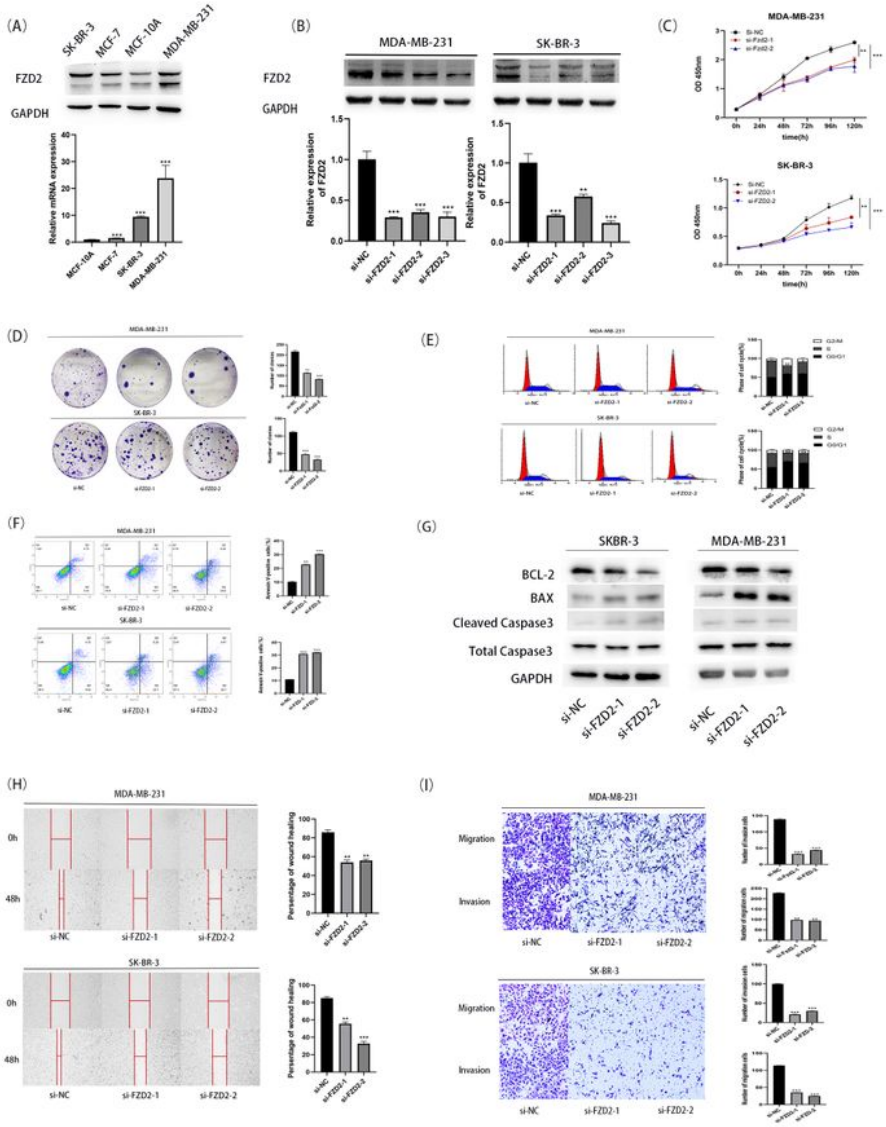

Figure 2

FZD2 is critical for BC cell cell growth, migration, invasion and apoptosis in vitro. (A) FZD2 mRNA and protein were measured at cellular levels. (B) Knockdown of FZD2 induced by specific siRNAs in MDA-MB-231 and SK-BR-3 cells was identified by qRT-PCR and western blot. (C) CCK-8 assay was implemented to assess cell growth after inhibition of FZD2 expression. (D) The number of colonies was quantified after siRNA transfection in two BC cells. (E) Cell cycle distribution was evaluated by flow cytometry in two BC cells with FZD2 silencing. (F) Flow cytometry analysis of apoptosis in BC cells transfected with si-NC or FZD2-specific siRNAs. (G) Western blot was conducted to detect apoptosis-related proteins in BC cells with FZD2 silencing. (H) Representative images and quantitative bar graphs of wound-healing distance for FZD2-silenced cells. (I) Representative micrographs and quantification of the invaded or migrated cells after FZD2 knockdown. Results were obtained from Matrigel-coated transwell assays and non-Matrigel-coated transwell assays. *p< 0.05, **p< 0.01, ***p< 0.001 were symbols of statistical significance.FZD2, frizzled class receptor 2; BC, breast cancer.

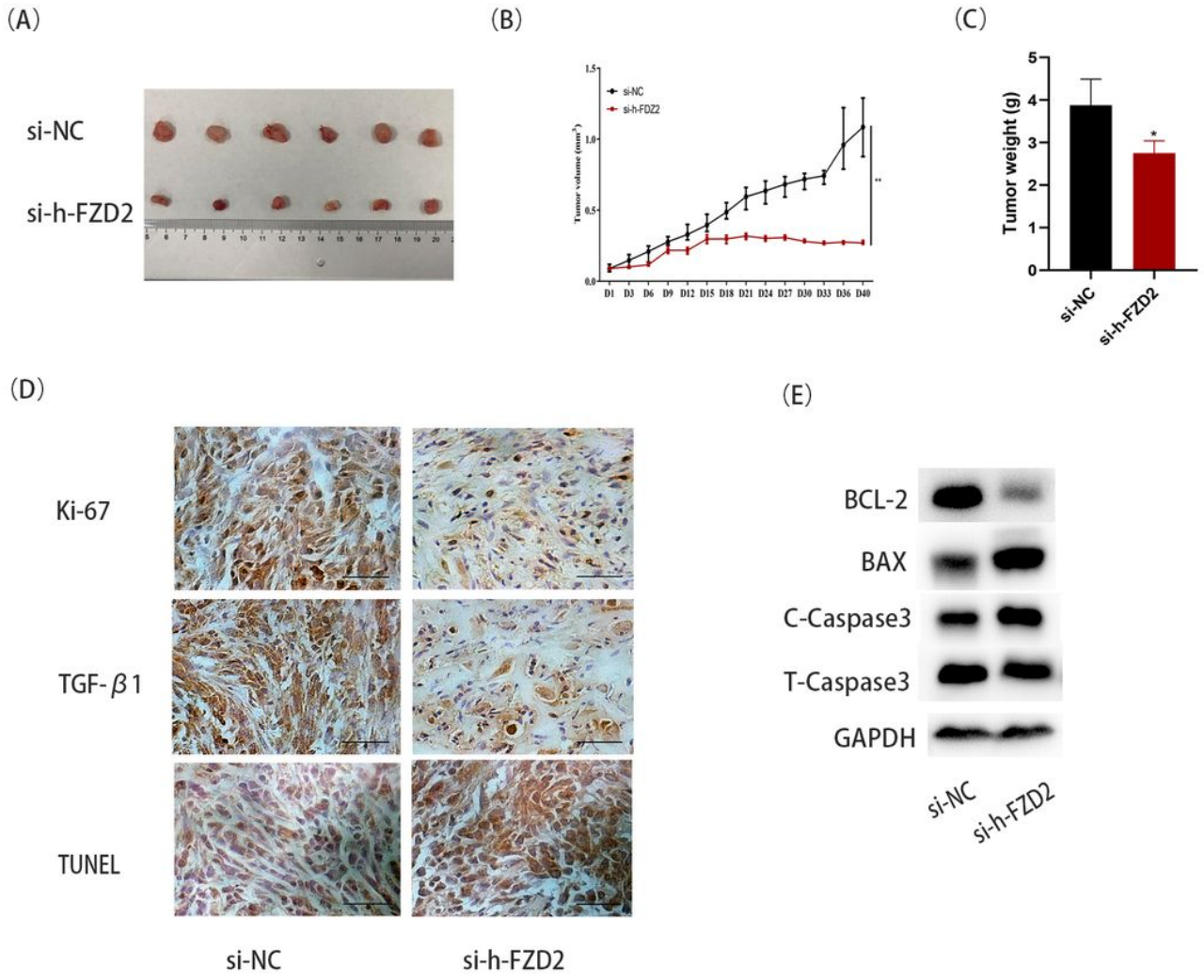

Figure 3

FZD2 promotes BC cell growth in vivo. (A) Images of tumors removed from two groups of mice were shown. (B) Volumes of tumors derived from FZD2-downregulated cells or control cells. (C) Weights of

tumors derived from FZD2-downregulated cells or control cells. (D) The positivity of FZD2, TGF-β1 and Ki-67 in the tumor tissues collected from two groups of mice was detected by IHC (Original magnification, ×400, scale bar = 100 μm).Apoptosis in the tissues collected from two groups of mice was measured by TUNEL assay. (E) Apoptosis-related proteins were detected in two groups of tumor tissues. *p< 0.05, **p< 0.01, ***p< 0.001 was a symbol of statistical significance. FZD2, frizzled class receptor 2; BC, breast cancer.

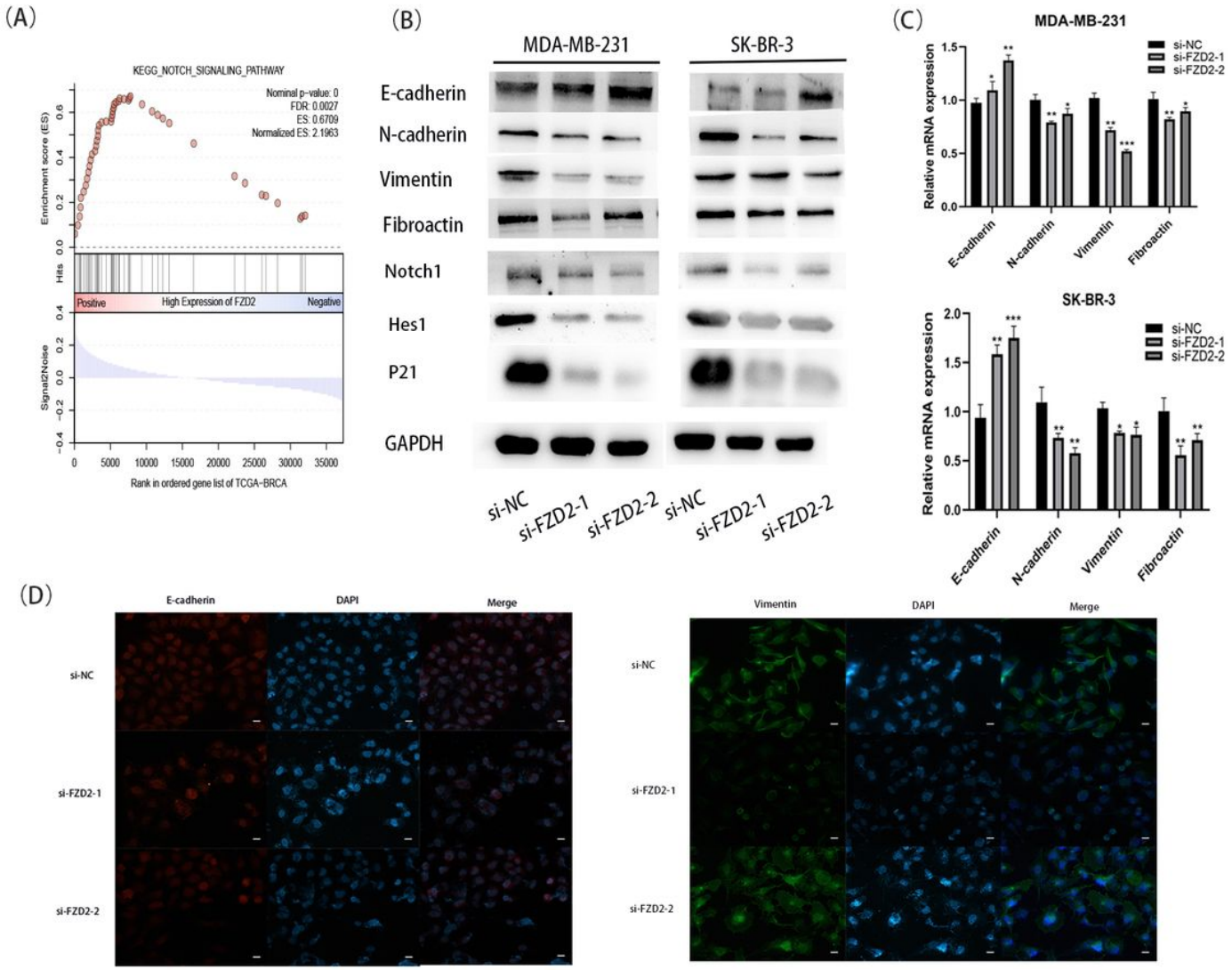

Figure 4

FZD2 induces EMT and regulates the activity of Notch signaling in BC cells. Two BC cells transfected with FZD2 siRNAs for 24 hwere harvested for the following studies. (A) GESA database shows the correlation between FZD2 expression and Notch signaling pathway. (B) EMT markers (E-cadherin, N-cadherin, Vimentin and Fibronectin) and Notch pathway factors (Notch1, P21 and Hes1) were examined by western blot in indicated BC cells. (C) EMT markers were detected by qRT-PCR at mRNA levels. (D) The intensity of E-cadherin and Vimentin was tested by immunofluorescence. *p< 0.05, **p< 0.01, ***p< 0.001 was a symbol of statistical significance. FZD2, frizzled class receptor 2; BC, breast cancer; EMT, epithelial-to mesenchymal transition.

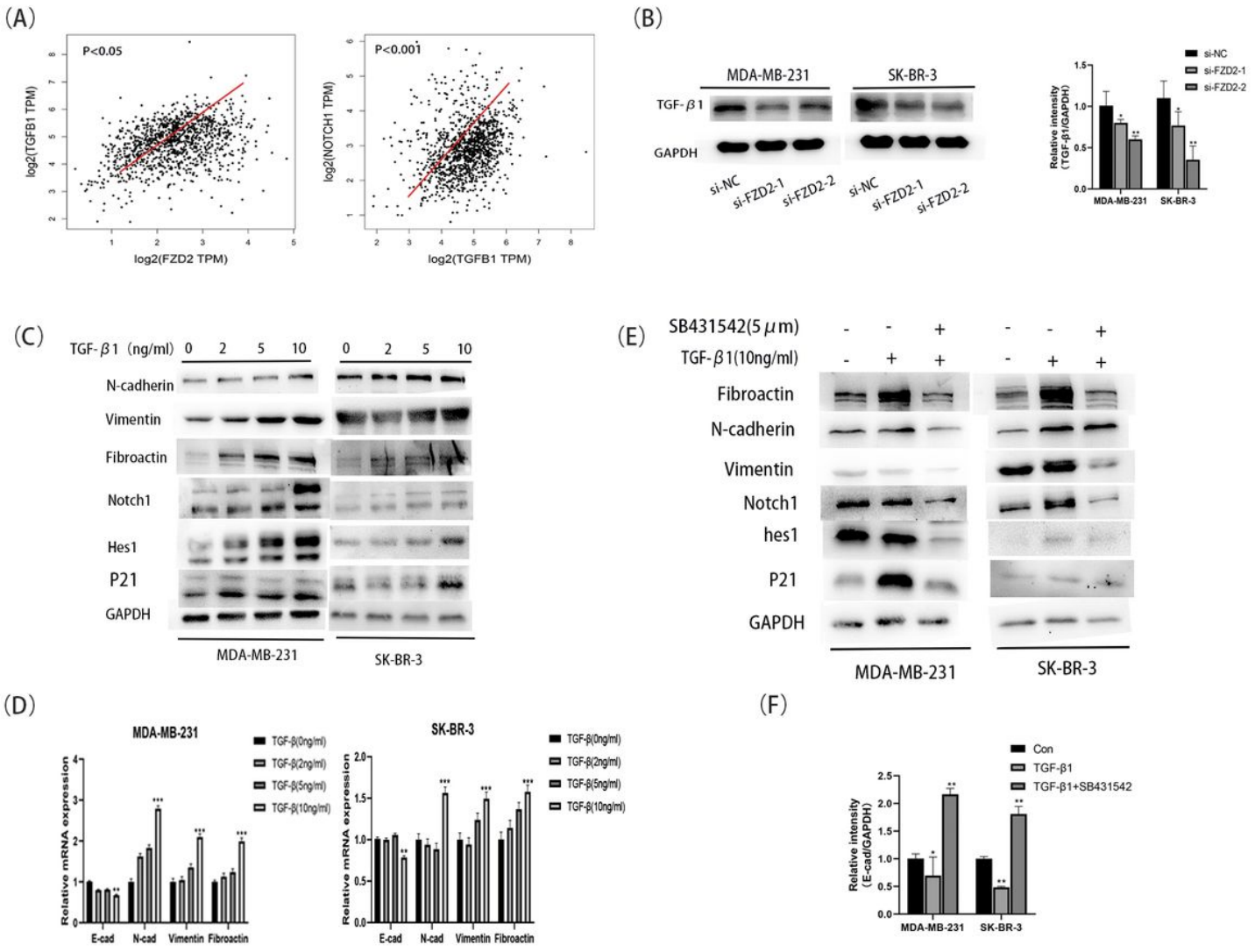

Figure 5

FZD2 positively regulates TGF-β1 expression in BC cells via Notch signaling pathway. (A) Expression correlation of TGF-β1 with FZD2 or Notch1 in BC patient samples was analyzed based on GEPIA database. (B) The protein level of TGF-β1 was measured in BC cells transfected with si-NC or FZD2-specific siRNAsfor 24 h. (C) EMT markers (E-cadherin, N-cadherin, Vimentin and Fibronectin) and Notch pathway factors (Notch1, P21 and Hes1) were tested in BC cells treated with TGF-β1 (0, 2, 5 and 10 ng/ml) for 24 h. (D) qRT-PCR was used to analyze the mRNA levels of EMT markers in TGF-β1-strengthened BC cells. (E) The levels of related proteins (E-cadherin, N-cadherin, Vimentin, Fibronectin, Notch1, Hes1, P21) were measured by western blot in BC cells pre-treated with SB431542 (5 μM) for 2 h, followed by TGF-β1 (10 ng/ml) incubation for another 24 h. (F) E-cadherinmRNA was subjected to qRT-PCRanalysis in BC cells treated with SB431542 and TGF-β1. *p< 0.05, **p< 0.01, ***p< 0.001 was a symbol of statistical significance. FZD2, frizzled class receptor 2; BC,breast cancer; EMT, epithelial-to mesenchymal transition, TGF-β1, transforming growth factor-β1.